Folate-Targeted Polymeric Nanoparticle Formulation of Docetaxel Is an Effective Molecularly Targeted Radiosensitizer with Efficacy Dependent on the Timing of Radiotherapy

Michael E. Werner,[†,‡,#] Jonathan A. Copp,[†,‡,#] Shrirang Karve,[†,‡] Natalie D. Cummings,[†,‡] Rohit Sukumar,[†,‡] Chenxi Li,[§] Mary E. Napier,[⊥] Ronald C. Chen,[∥] Adrienne D. Cox,[∥] and Andrew Z. Wang[†,‡,*]

[†]Laboratory of Nano- and Translational Medicine, Department of Radiation Oncology, Lineberger Comprehensive Cancer Center, University of North Carolina—Chapel Hill, Chapel Hill, North Carolina, United States, [‡]Carolina Center for Cancer Nanotechnology Excellence, University of North Carolina—Chapel Hill, Chapel Hill, North Carolina, United States, [§]Department of Biostatistics and NC TraCS Institute, University of North Carolina—Chapel Hill, Chapel Hill, North Carolina, United States, [⊥]Department of Biochemistry and Biophysics, Lineberger Comprehensive Cancer Center, University of North Carolina—Chapel Hill, Chapel Hill, North Carolina, United States, and, [∥]Department of Radiation Oncology, Lineberger Comprehensive Cancer Center, University of North Carolina—Chapel Hill, Chapel Hill, North Carolina, United States. [#]These authors contributed equally to this work.

ABSTRACT

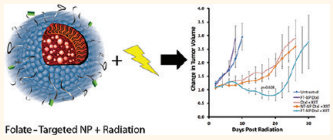

Nanoparticle (NP) chemotherapeutics hold great potential as radiosensitizers. Their unique properties, such as preferential accumulation in tumors and their ability to target tumors through molecular targeting ligands, are ideally suited for radiosensitization. We aimed to develop a molecularly targeted nanoparticle formulation of docetaxel (Dtxl) and evaluate its property as a radiosensitizer. Using a biodegradable and biocompatible lipid-polymer NP platform and folate as a molecular targeting ligand, we engineered a folate-targeted nanoparticle (FT-NP) formulation of Dtxl. These NPs have sizes of 72 ± 4 nm and surface charges of −42 ± 8 mV. Using folate receptor overexpressing KB cells and folate receptor low HTB-43 cells, we showed folate-mediated intracellular uptake of NPs. *In vitro* radiosensitization studies initially showed FT-NP is less effective than Dtxl as a radiosensitizer. However, the radiosensitization efficacy is dependent on the timing of radiotherapy. *In vitro* radiosensitization conducted with irradiation given at the optimal time (24 h) showed FT-NP Dtxl is as effective as Dtxl. When FT-NP Dtxl is compared to Dtxl and nontargeted nanoparticle (NT-NP) Dtxl *in vivo*, FT-NP was found to be significantly more effective than Dtxl or NT-NP Dtxl as a radiosensitizer. We also confirmed that radiosensitization is dependent on timing of irradiation *in vivo*. In summary, FT-NP Dtxl is an effective radiosensitizer in folate-receptor overexpressing tumor cells. Time of irradiation is critical in achieving maximal efficacy with this nanoparticle platform. To the best of our knowledge, our report is the first to demonstrate the potential of molecularly targeted NPs as a promising new class of radiosensitizers.

KEYWORDS: nanomedicine · nanoparticle · chemoradiotherapy · radiosensitization · folate-targeted

Radiosensitization, the use of agents to improve cancer cells' sensitivity to radiotherapy, has been an important concept in cancer treatment. It is the main concept behind concurrent administration of chemotherapy and radiotherapy (chemoradiotherapy), which is a standard treatment regimen for many cancers including head and neck, lung, esophageal, gastric, rectal, anal, and cervical cancers.[1] Current clinical radiosensitizers are mainly comprised of chemotherapeutics. Among them, docetaxel (Dtxl) is one of the more effective radiosensitizers.[2−4] A major limitation of docetaxel is its poor solubility in water and its need for a solvent (polysorbate-80) for clinical administration. Since polysorbate-80 has many undesirable side effects, including hypersensitivity reactions, there has been intense interest in developing alternative formulations of docetaxel.[5]

Recent advances in nanomedicine have led to the development of nanoparticle formulations of docetaxel.[6] Nanoparticle therapeutic carriers are well suited for the treatment of cancers, as they take advantage of the enhanced permeability and retention (EPR) effect and preferentially accumulate in tumors.[7] Furthermore, these nanoparticles can be actively targeted to tumor cells through molecular targeting ligands. Thus, these nanoparticle formulations of docetaxel have significant clinical potential for improving the efficacy and lowering the toxicity of docetaxel. Indeed, many preclinical studies have demonstrated the efficacy of nanoparticle formulations of docetaxel for cancer treatment, which also enabled the rapid translation of this technology.[8−17] BIND-014, a molecular targeted polymeric nanoparticle formulation of docetaxel, has recently entered phase I clinical trial testing.[18]

In addition to functioning as chemotherapeutics, nanoparticles also have the potential

* Address correspondence to andrew_wang@med.unc.edu.

Received for review August 17, 2011 and accepted October 19, 2011.

Published online October 19, 2011
10.1021/nn203165z

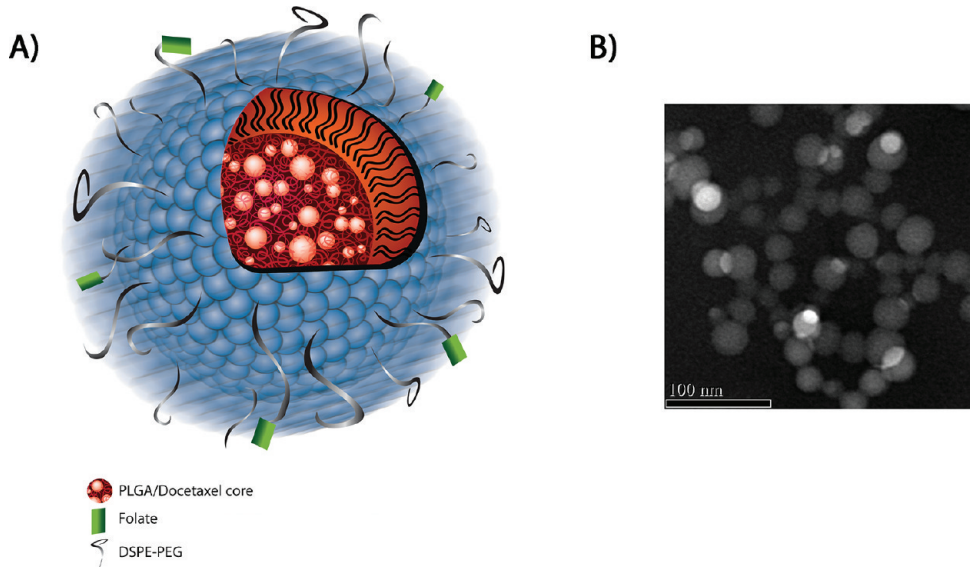

Figure 1. Characterization of NP. (A) Depiction of NP. (B) TEM image of NP Dtxl showing monodisperse particles with a narrow size distribution of 70 ± 10 nm.

to be excellent radiosensitizers. Unlike small-molecule chemotherapeutics, which are broadly distributed in malignant and normal tissue, the latter causing treatment-related toxicity, nanoparticles' unique biodistribution, preferential accumulation in tumors, and poor penetration in nearby normal tissues are ideal for a radiosensitizer. Nanoparticles could potentially improve the efficacy of radiotherapy in the tumor and reduce the toxicity of nearby normal organs when compared to their small-molecule counterparts. Despite their high potential as radiosensitizers, there is currently no preclinical study evaluating the potential of nanoparticle docetaxel as a radiosensitizer and limited data overall exploring the use of any nanoparticle chemotherapeutics as radiosensitizers.[19−21]

In this study, we evaluated nanoparticle formulations of docetaxel as radiosensitizers. To accomplish this goal, we engineered a biodegradable and biocompatible polymeric nanoparticle formulation of docetaxel. To potentially further improve its efficacy, we also developed a molecular targeted nanoparticle formulation of docetaxel. We utilized head and neck cancer (HNSCC) as a model, for which chemoradiotherapy is the standard of care for advanced disease. Folate was chosen as a targeting ligand for the development of molecular targeted nanoparticles, as folate receptor (FR) has been shown to be frequently overexpressed in HNSCC tumors. Furthermore, increased FR expression has been correlated with poor survival.[22,23] We validated that folate can mediate the specific uptake of nanoparticles by folate-receptor-overexpressing tumor cells. We then evaluated the radiosensitization efficacy of folate-targeted NP Dtxl (FT-NP Dtxl) and nontargeted NP Dtxl (NT-NP Dtxl) in both FR-overexpressing and FR-deficient HNSCC tumor cells *in vitro*. We also evaluated the effects of timing between NP Dtxl administration and radiotherapy on the efficacy of radiosensitization. Lastly, we compared the efficacy of FT-NP Dtxl, NT-NP Dtxl, and Dtxl as radiosensitizers and the importance of timing with radiotherapy *in vivo* using a murine xenograft model.

RESULTS

Formulation and Characterization of NT-NP Dtxl and FT-NP Dtxl. For this study we utilized a biocompatible biodegradable polymer based nanoparticle platform.[24] The particle is composed of a biodegradable polymeric (PLGA) core, which can encapsulate hydrophobic chemotherapeutics such as Dtxl. The NP surface is composed of lipids (lecithin) and lipid-PEG, which prevents protein adsorption (DSPE-PEG) (Figure 1A). Nontargeted NPs (NT-NPs) were found to have sizes of 70 ± 10 nm, confirmed by TEM (Figure 1B). Their surface charges (ζ potential) were −40 ± 5 mV and have a polydispersity of 0.15 ± 0.05. To engineer folate-targeted NPs, we incorporated DSPE-PEG-folate into the nanoparticle surface. The hydrophobic lipid tail domain of DSPE-PEG-folate interacts with the hydrophobic domains of lecithin and allows self-assembly of DSPE-PEG-folate onto the particle surface (Figure 1A). Characterization of folate-targeted NPs (FT-NPs) demonstrated sizes of 72 ± 4 nm, ζ potential of −42 ± 8 mV and a polydispersity of 0.16 ± 0.05. Dtxl was encapsulated in the NP at 5 wt % of the polymer with an encapsulation efficiency of 40 ± 7%. Dtxl release profiles were characterized in both NT-NP Dtxl and FT-NP Dtxl. Both particles demonstrated controlled drug release kinetics, and 95% of the drug was released from the nanoparticles at 24 h. Also, there was no significant difference between the two formulations (Figure 2).

FT-NPs Have Higher Intracellular Uptake than NT-NPs by Folate Receptor Overexpressing KB Cells than in Non-overexpressing HTB-43 Cells. To demonstrate that the folate targeting ligand can increase target specific NP uptake, we compared NP uptake in KB cells, which overexpress the alpha isoform of the folate receptor (FR), to that in HTB-43 cells, which do not. FRα expression levels were confirmed by Western blot (Figure 3A). FT-NP and NT-NPs encapsulating fluorescent cholesterol were incubated with these cells *in vitro*. As shown in Figure 3B, minimal fluorescence was seen in HTB-43 cells with either nontargeted or targeted NP, indicating minimal nonspecific uptake. Similarly, nontargeted NPs were not taken up efficiently in KB cells. In contrast, FT-NPs were readily taken up by FR-overexpressing KB cells, as indicated by the intense fluorescence.

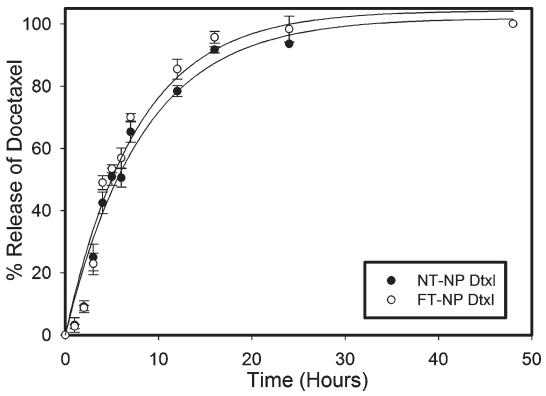

Figure 2. NP-Dtxl release profiles in phosphate buffer at 37 °C. NT-NP Dtxl and FT-NP Dtxl show first-order controlled drug release. There is no significant difference in release kinetics between the two formulations. Error bars correspond to standard deviations of repeated measurements (two NP preparations, three samples per time point).

To further verify folate-mediated uptake, KB and HTB-43 cells were also treated with FT-NP Dtxl or NT-NP Dtxl and lysed to examine the uptake of Dtxl. As seen in Figure 3C, KB cells treated with FT-NP Dtxl show greater percent uptake of Dtxl compared to NT-NP Dtxl-treated cells, whereas HTB-43 shows no difference between FT-NP Dtxl and NT-NP Dtxl uptake. These results support a FR-dependent mechanism for FT-NP uptake.

Comparative Radiosensitization of Dtxl, NT-NP Dtxl, and FTNP Dtxl *in Vitro*. We compared radiation responses in the presence of targeted and nontargeted NP Dtxl to that of free, unencapsulated Dtxl (polysorbate formulation) *in vitro*. To determine the proper dose of each Dtxl formulation, we obtained dose–response curves for each therapeutic at 0 Gy (Supplemental Figure 1). We then conducted radiosensitization experiments using

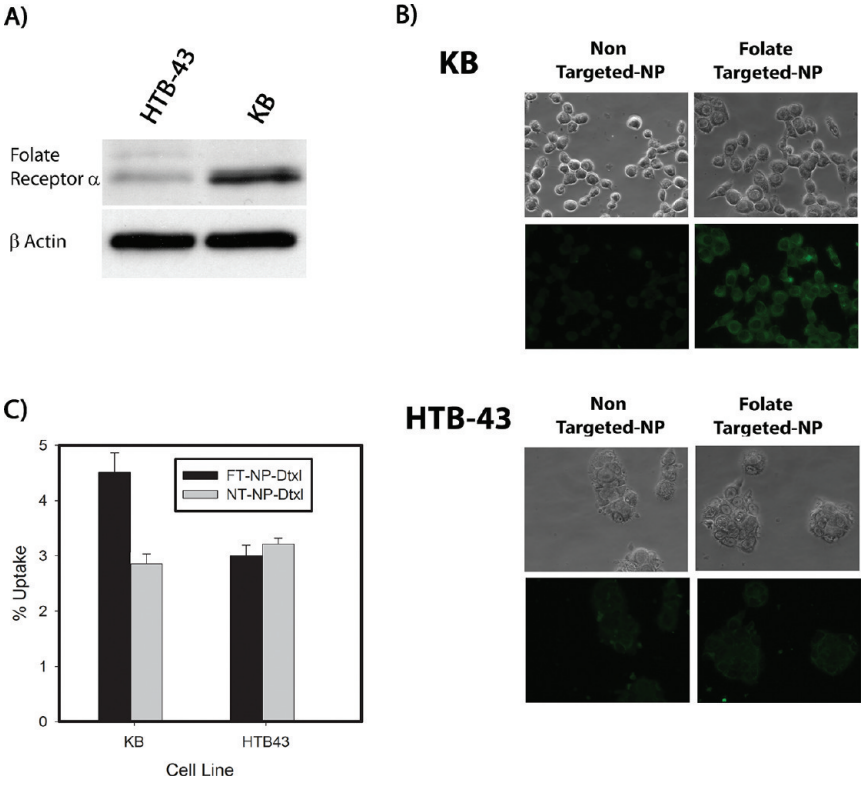

Figure 3. Intracellular uptake of folate-targeted NP is greater than NT-NP and is dependent on expression of the folate receptor. (A) Endogenous expression of folate receptor α in KB and HTB43 cells. (B) Representative immunofluorescent images of KB and HTB-43 cells treated with NPs containing fluorescent cholesterol demonstrate greater uptake of folate-targeted NPs (right) compared to an equal amount of NT-NP on the left in KB cells, which robustly express folate receptor α. In contrast, there is minimal uptake of either targeted or nontargeted NPs in HTB-43 cells, which express low levels of the receptor. (C) Dtxl was measured in KB or HTB-43 cell lysates treated with FT-NP Dtxl or NT-NP Dtxl. KB cells treated with FT-NP Dtxl had the highest uptake. Error bars correspond to standard deviations of repeated measurements.

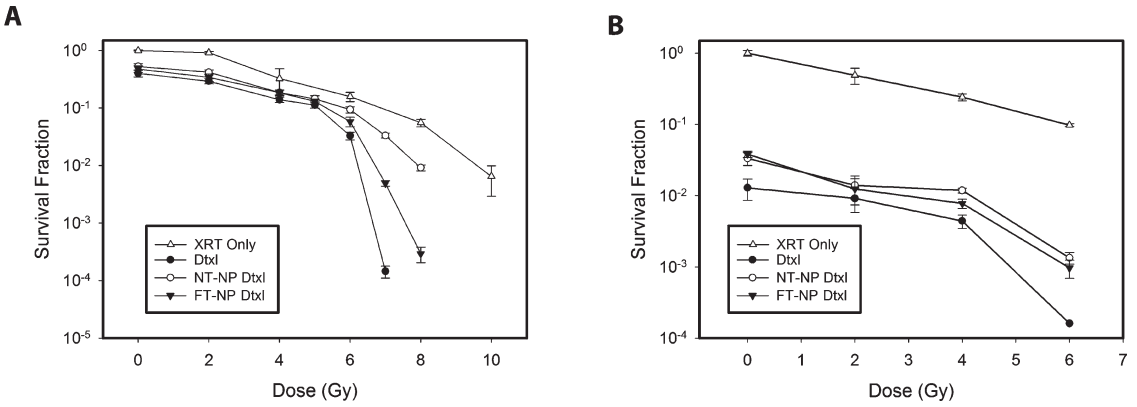

Figure 4. Efficacy of folate-targeted NP as a radiosensitizer. Clonogenic survival assays of KB (A) or HTB-43 (B) cells treated with radiation alone or with Dtxl, NT-NP Dtxl, or FT-NP Dtxl and the indicated dose of radiation 3 h after NP treatment. The error bars correspond to standard deviations of repeated measurements (two NP preparations, three samples per time point).

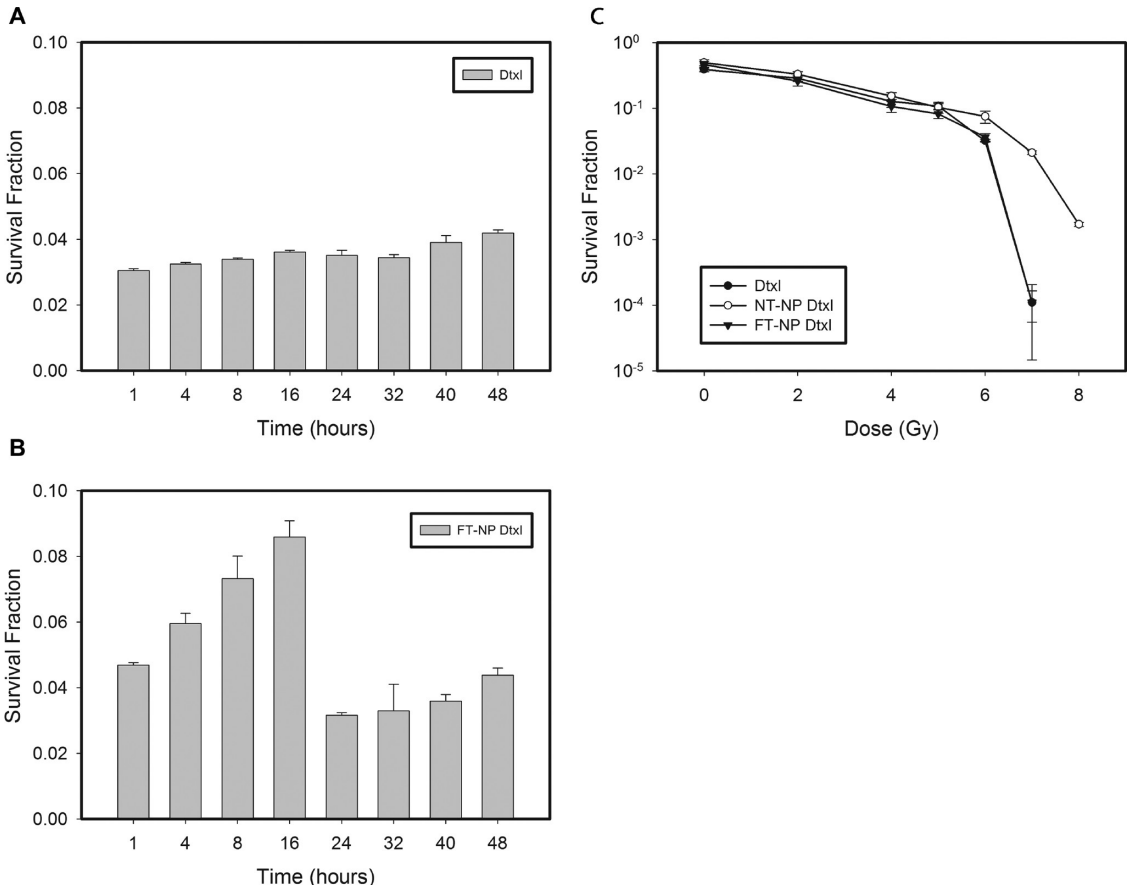

Figure 5. Timing of irradiation alters efficacy of FT-NP Dtxl *in vitro*. Graph of surviving fraction from clonogenic survival assays of KB cells treated with Dxtl (A) or FT-NP Dtxl (B) irradiated with 4 Gy at the indicated times. (C) Clonogenic survival assay of KB cells treated with Dtxl, NT-NP Dtxl, or FT-NP Dtxl and the indicated amount of radiation 24 h post-treatment. Error bars correspond to standard deviations of repeated measurements (two separate runs, three samples per time point).

the IC_{50} concentrations of FT-NP Dtxl and NT-NP Dtxl (1.25 uM) and/or Dtxl (0.65 uM) with irradiation occurring 3 h after Dtxl treatment. As seen from the clonogenic survival curves depicted in Figure 4A, FT-NP Dtxl was significantly more effective than NT-NP Dtxl and is nearly as effective as free Dtxl in KB cells. In contrast, NT-NP Dtxl was considerably less effective, which was expected due to its poor uptake compared to FT-NP Dtxl (Figure 3B). Also as expected, given the lack of uptake in HTB-43 cells of either NT-NP Dtxl or FT-NP Dtxl (Figure 3B), there was no difference in post-radiation survival between these therapeutics, and neither effectively reduced survival in these cells compared to free Dtxl (Figure 4B). Together with the data in Figure 3B, these results indicate that a molecularly targeted NP formulation of Dtxl that can be taken up selectively by

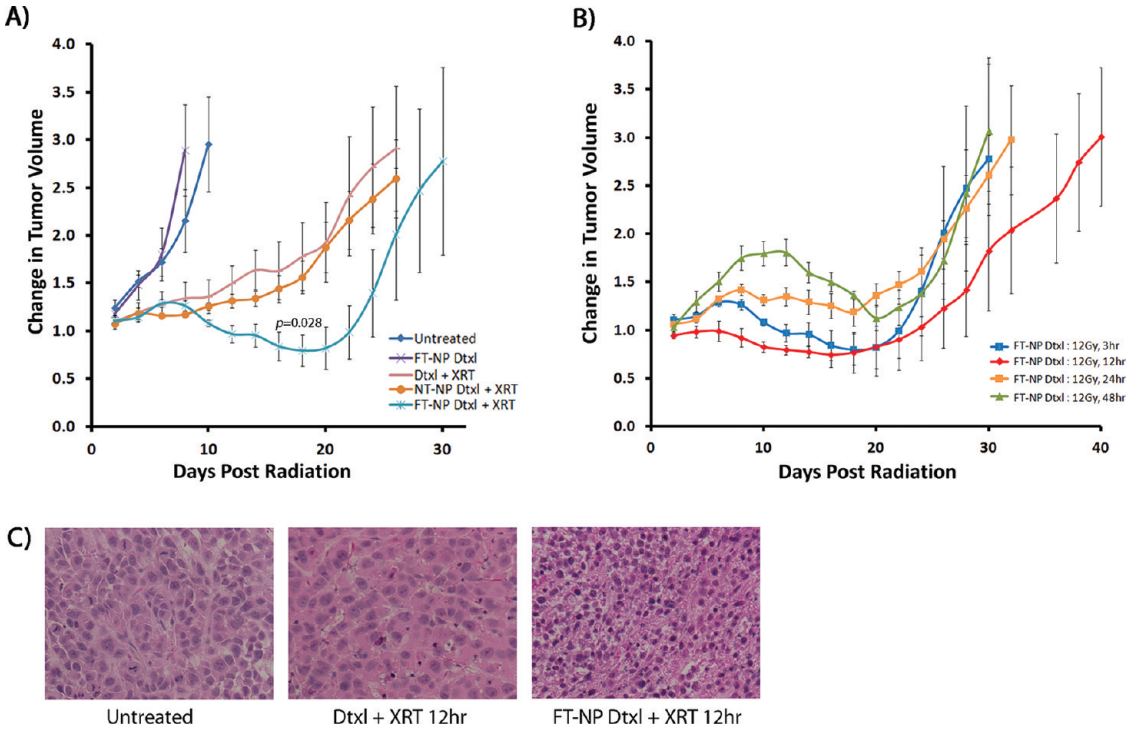

Figure 6. Timing of irradiation alters efficacy of FT-NP Dtxl *in vivo*. KB tumors were established in mice. (A) Mice were left untreated or treated with 2 mg/kg of Dtxl iv (as either polysorbate-Dtxl, NT-NP Dtxl, or FT-NP Dtxl) ± 12 Gy of irradiation 3 h post-injection. Change in tumor volume was measured. (B) Mice were treated with 2 mg/kg of FT-NP Dtxl iv + 12 Gy of irradiation at either 3, 12, 24, or 48 h post-injection. Change in tumor volume was measured. (C) Representative histology of polysorbate-Dtxl- or FT-NP Dtxl-treated KB tumors irradiated 12 h post-injection.

FR-overexpressing tumor cells is capable of inducing a response in irradiated cells similar to that of free Dtxl, a known radiosensitizer that unfortunately also induces significant toxicity in non-FR-overexpressing normal cells.

Optimal Timing of Radiotherapy with FT-NP Dtxl Is 24 h after Incubation. A key issue in identifying the most effective chemoradiation strategies is optimizing the timing to deliver the individual components of combined treatments relative to each other. We speculated that delayed release of Dtxl from the NPs might require a longer optimal treatment time for encapsulated Dtxl *vs* free Dtxl, which is bioavailable immediately. To determine whether and how the timing of radiotherapy can affect the efficacy of radiosensitization with NP Dtxl, we performed clonogenic survival assays on KB cells incubated with FT-NP Dtxl when radiation was given at different times after drug administration. KB cells were incubated with FT-NP Dtxl or free Dtxl and irradiated with 4 Gy at 1, 4, 8, 16, 24, 32, 40, or 48 h after incubation. As expected, treatment with free Dtxl resulted in the lowest survival fraction when radiation was given at early time points following drug administration. The optimal time point tested for radiation was apparently the earliest, at 1 h post-treatment, with a slow rise over time, presumably as the drug became less effective due to metabolic clearance (Figure 5A). In contrast, FT-NP Dtxl treatment resulted in a dramatically lower survival when longer times separated drug treatment and radiation (Figure 5B). The unexpected sharp drop-off between 16 and 24 h suggests that the basis for poorer tumor cell survival at 24 h and later is unlikely to be explained simply by altered bioavailability of drug in the encapsulated formula compared to free drug. Using the optimal 24 h time point, we then reassessed relative post-radiation survival of KB cells upon treatment with FT-NP Dtxl, NT-NP Dtxl, or Dtxl *in vitro*. When radiotherapy was given at 24 h post-drug treatment, FT-NP Dtxl was as effective as Dtxl *in vitro* (Figure 5C).

Radiosensitization Efficacy of Dtxl, NT-NP Dtxl, and FT-NP Dtxl *in Vivo*. We next compared the efficacy of NT-NP Dtxl and FT-NP Dtxl against Dtxl in an *in vivo* tumor model. Mice bearing KB cell xenograft tumors were treated with Dtxl, NT-NP Dtxl, or FT-NP Dtxl and subsequently irradiated 3 h after treatment. As seen in Figure 6A, all of the Dtxl formulations led to significant tumor growth delay when tumors were irradiated, but FT-NP Dtxl produced the maximum tumor growth delay and was significantly different from NT-NP Dtxl ($p = 0.028$). A control group of Dtxl was also preformed, but the change in tumor volume was not statistically different from the FT-NP Dtxl group (data not shown). We next determined whether the timing of irradiation also affects radiosensitization efficacy of FT-NP Dtxl *in vivo*. We irradiated tumor-bearing mice at 3, 12, 24, and 48 h after administration of FT-NP Dtxl. As seen in Figure 6B, mice that were irradiated 12 h after systemic treatment with FT-NP Dtxl displayed the most tumor growth delay ($P = 0.03$ at day 18, compared to 48 h treatment).

The irradiated tumors were also analyzed for treatment response. As seen in Figure 6C, tumors treated with FT-NP Dtxl and irradiated 12 h after systemic treatment consistently demonstrated more cell death, evidenced by increased number of cells with condensed nuclei, compared to that of Dtxl. These data demonstrate that FT-NP Dtxl is a better radiosensitizer *in vivo* than either Dtxl or NT-NP Dtxl. Furthermore, the timing of irradiation after systemic treatment is critical in determining maximal efficacy.

CONCLUSION

The next generation of NP chemotherapeutics is being translated into clinical practice, representing an exciting new class of radiosensitizers. However, there is a general lack of preclinical data or clinical data on how to utilize NP therapeutics in radiosensitization given their unique properties. There are currently two nanoparticle formulations of chemotherapeutics aside from liposomes in clinical practice. Abraxane, a nanoparticle formulation of albumin and paclitaxel, has been evaluated in one preclinical study and is being evaluated as a radiosensitizer in several ongoing trials.[21,25] The other nanoparticle chemotherapeutic, Genexol-PM, is a polymeric nanoparticle formulation of paclitaxel that has not been studied as a radiosensitizer. Furthermore, despite the many studies on molecularly targeted nanoparticles for cancer treatment, there has been no report on the utilization of molecularly targeted nanoparticles as radiosensitizers. In this study, we report the first preclinical evidence on using a folate-targeted nanoparticle formulation of docetaxel as a radiosensitizer.

Among the different nanoparticle platforms, there has been intense interest in the clinical development of polymeric NPs due to their relative higher stability, ability to carry hydrophobic cargos, and controlled drug release profile. It is an ideal nanoparticle platform for the delivery of taxanes, such as docetaxel. Therefore, we engineered a biodegradable biocompatible polymeric NP to deliver Dtxl. This platform consists of materials that are considered safe by the Food and Drug Administration (FDA).[26,27] NP characterization studies showed our nanoparticle has excellent properties as a drug delivery vehicle: a narrow size distribution near 70 nm, negative surface charge, and controlled drug release. In addition, these characteristics are consistent with other polymer NP formulations including commercial formulations of Genexol-PM and BIND-004.[28,29] It is important to note that the addition of the targeting ligand (folate) did not significantly change the particle size, charge, or drug release profile.

Previous studies have demonstrated that targeting ligands can promote intracellular uptake of NPs, leading to higher intracellular drug accumulation within cancer cells.[30,31] This increased therapeutic concentration can in turn lead to increased radiosensitization. In this study, we confirmed that incorporation of a folate targeting ligand can lead to enhanced, and presumably folate-receptor-mediated, intracellular uptake of NPs in tumor cells overexpressing the folate receptor. We also demonstrated that nontargeted NPs had minimal nonspecific uptake, highlighting the importance and utility of biological targeting. However, we were surprised by the apparently lower initial radiosensitization efficacy of FT-NP Dtxl when compared to Dtxl at its IC_{50} concentration. Since polymeric nanoparticles release drug in a controlled fashion, different than that of small-molecule chemotherapeutics, we hypothesized that the controlled drug release may affect the timing of radiotherapy to achieve the maximal radiosensitization. A previous report has also suggested radiosensitization efficacy depends on the timing of irradiation with nanoparticle-albumin-bound paclitaxel (nab-paclitaxel).[21] Therefore, we studied the radiosensitization efficacy of FT-NP Dtxl with radiotherapy given at different time points after drug incubation. Indeed, we observed that the time point for maximal radiosensitization with FT-NP Dtxl was 24 h, in contrast to 1 h for Dtxl. This finding was confirmed by repeating higher *in vitro* radiosensitization with radiotherapy given at 24 h post-drug incubation. Although the 24 h time point corresponded to the time where the majority of the drug (95%) has been released from the NPs, it does not fully explain the difference between 24 h and the other time points such as 16 h or the dramatic decrease in survival between time points at 16 h and earlier *vs* 24 h and later. Further studies are under way to explain such differences.

Lastly, we studied the comparative efficacy of Dtxl, NT-NP Dtxl, and folate-targeted NP Dtxl as radiosensitizers *in vivo*. Using murine xenografts of KB cells, we were able to demonstrate that FT-NP Dtxl was more effective as a radiosensitizer than Dtxl and NT-NP Dtxl, highlighting the importance of biological targeting. Even though FT-NP Dtxl had the same efficacy as Dtxl *in vitro*, its *in vivo* efficacy may have been enhanced by the unique properties of nanoparticles, such as EPR and molecular targeting. In addition, we confirmed that radiosensitization efficacy was dependent on timing of radiotherapy in the *in vivo* setting as well. In this *in vivo* experiment, irradiation at 12 h post-drug administration produced the maximum radiosensitization. The difference in optimal time of irradiation between *in vitro* and *in vivo* is likely due to the inherent differences in pharmacokinetics and tumor cell biology between *in vitro* and *in vivo* experimental systems. Also, around 20 d post-treatment, we see a rapid increase in the change in tumor volume. This is most likely a result of a phenomenon known as accelerated repopulation.[32,33] Briefly, in this process the few tumors cells surviving the initial chemo- or radiotherapeutic treatment demonstrate an ability to repopulate the damaged tumor at an accelerated rate. The molecular mechanisms for accelerated repopulation are still emerging.[34]

Nonetheless, we have demonstrated that timing of irradiation can be critical to the efficacy of radiosensitization. Given the similar finding on nab-paclitaxel, this suggests a potential unique property to nanoparticle formulations of taxanes. Nanoparticle taxanes are poised to be evaluated as radiosensitizers in clinical trials; the success of these trials can depend on our full understanding of the optimal timing of irradiation. Our laboratory has initiated studies to elucidate potential mechanisms for the timing dependence of FT-NP Dtxl. Overall, the data suggest that there is an optimal time for radiosensitization for each NP platform. Such information will be crucial in clinical trial design of radiosensitization using NP therapeutics.

In conclusion, a folate-targeted nanoparticle formulation of Dtxl is an effective radiosensitizer in folate-receptor-overexpressing head and neck tumor cells. Time of irradiation can be critical in achieving maximal efficacy with this nanoparticle platform. To the best of our knowledge, this study is the first to demonstrate the potential of molecularly targeted NPs as a promising new class of radiosensitizers. Our comprehensive *in vitro* and *in vivo* characterization of the FT-NP Dtxl and findings provide rationale for its further study for clinical development. Further, our finding on the time-dependent radiosensitization may apply to other types of nanoparticles with controlled drug release.

MATERIALS AND METHODS

Materials. All chemicals were obtained from Sigma-Aldrich (St. Louis, MO, USA) unless otherwise noted. PLGA (poly(D,L-lactide-*co*-glycolide)) with a 50:50 monomer ratio, ester-terminated, and viscosity of 0.72−0.92 dL/g was purchased from Durect Corporation (Pelham, AL, USA). Soybean lecithin consisting of 90−95% phosphatidylcholine was obtained from MP Biomedicals (Solon, OH, USA). DSPE−PEG2000−COOH (1,2-distearoyl-*sn*-glycero-3-phosphoethanolamine-*N*-carboxy-(polyethylene glycol) 2000) and DSPE−PEG2000−Folate (1,2-distearoyl-*sn*-glycero-3-phosphoethanolamine-*N*-carboxy-(polyethylene glycol) 2000-Folate) were obtained from Avanti Polar Lipids (Alabaster, AL, USA).

Formulation and Characterization of NP Docetaxel. PLGA−lecithin−PEG core−shell NPs were synthesized from PLGA, soybean lecithin, and DSPE−PEG−COOH using a previously reported nanoprecipitation technique.[24] Briefly, PLGA was dissolved in acetonitrile at a concentration of 1 mg/mL. To generate folate-targeted NPs, (lecithin)/(DSPE−PEG + DSPE−PEG−Folate) (7:3 molar ratio) with a weight ratio of 15% to the PLGA polymer was dissolved in 4% ethanol aqueous solution and heated to 56 °C. The PLGA/acetonitrile solution was then added dropwise to the heated aqueous solution under gentle stirring followed by 3 min of vortexing. The nanoparticles were allowed to self-assemble for 2 h with continuous stirring under vacuum. The NP solution was washed twice using an Amicon Ultra-4 centrifugal filter (Millipore, Billerica, MA, USA) with a molecular weight cutoff of 20 kDa and then resuspended in an equal volume of 2× PBS to obtain a final desired concentration. The NPs were used immediately. NP size (diameter, nm) and surface charge (ζ-potential, mV) were obtained with a ZetaPALS dynamic light scattering detector (Brookhaven Instruments Corporation, Holtsville, NY, USA). Transmission electron microscopy (TEM) images were obtained at the Microscopy Services Laboratory Core Facility at the UNC School of Medicine.

NP Dtxl Formulation, Characterization, and Release. To prepare drug-encapsulated NPs, Dtxl at a dosage of 10% (w/w) of the polymer was dissolved into the PLGA/acetonitrile solution before nanoprecipitation. To measure the drug loading yield and release profile of Dtxl, 3 mL of NP solutions at a concentration of 0.5 mg/mL was split equally into 30 Slide-ALyzer MINI dialysis microtubes with a molecular weight cutoff of 10 kDa (Pierce, Rockford, IL, USA) and subject to dialysis against 4 L of phosphate-buffered saline (PBS) with gentle stirring at 37 °C. PBS was changed periodically during the dialysis process. At the indicated times, 0.1 mL of solution from three microtubes was removed and mixed with an equal volume of acetonitrile to dissolve the NPs. Dtxl content was subjected to quantitative analysis using an Agilent 1100 HPLC (Palo Alto, CA, USA) equipped with a C18 chromolith flash column (Merck KGaA Darmstadt, Germany). Dtxl absorbance was measured by an UV−VIS detector at 227 nm and a retention time of 1.5 min in 0.25 mL/min 50:50 acetonitrile/water nongradient mobile phase.

Cell Culture. KB cells were acquired from the Tissue Culture Facility at the Lineberger Comprehensive Cancer Center at UNC. The HTB-43 cells were obtained from ATCC (Manassas, VA, USA). KB cells were cultured in folate-free RPMI 1640 (Gibco, Invitrogen, Carlsbad, CA, USA) supplemented with 10% fetal bovine serum (Mediatech, Manassas, VA, USA) and penicillin/streptomycin (Mediatech). HTB-43 cell were cultured in MEM (Cellgro) supplemented with 10% fetal bovine serum (Mediatech) and penicillin/streptomycin (Mediatech).

Fluorescence Microscopy. NPs were prepared as above with the addition of 4 ug of TopFluor cholesterol (Avanti Polar Lipids) to the PLGA/acetonitrile solution. KB and HTB-43 cells were grown in chamber slides (LABTEK-II) and treated with 140 ug/mL of FT-NP or NT-NP for 1 h and washed three times with PBS. Cells were fixed with 3.7% paraformaldahyde, permeabilized with 0.5% Triton X-100, and washed three times with PBS. Coverslips were mounted on the chamber slide with Prolong Gold (Molecular Probes, Invitrogen, Carlsbad, CA) for microscopy. Images were acquired with an IX 81 microscope (Olympus) and an ORCA-R2 camera (Hamamatsu Photonics K.K.) at the Microscopy Services Laboratory Core Facility at the UNC School of Medicine.

Western Blots. Whole cell lysates were generated using HNTG lysis buffer. Lysates were separated on 10% polyacrylamide gels (Biorad) and transferred to PVDF (Millipore) for immunoblotting. Anti-α-tubulin (Sigma) and anti FRα (Genetex) were used as primary antibodies, and goat anti-rabbit-HRP (Cell Signaling) was used as a secondary Ab.

Dose Response. Cells were seeded at 10 000 cells/well in a 96-well plate format. Cells were treated with therapeutics for 1 h and washed two times with PBS after incubation. Normal growth media was replaced. After 24 h, an MTS assay (3-(4,5-dimethylthiazol-2-yl)-5-(3-carboxymethoxyphenyl)-2-(4-sulfophenyl)-2*H*-tetrazolium, inner salt) (Promega, Madison, WI, USA) was performed per the manufactures instructions. Cell viability was measured on a Biotek Synergy 2 plate reader (Winooski, VT, USA).

Drug Uptake. Cells were treated at 70% confluency in a 10 cm dish with therapeutics for 1 h and washed two times with PBS after incubation. Cells were trypsinized and counted. The cell pellet was lysed with a 1:1 mixture of H_2O and MeOH, and lysate was separated *via* centrifugation. The supernatant was analyzed for Dtxl *via* HPLC.

***In Vitro* X-ray Irradiation.** The irradiation was produced by an Precision X-RAD 320 (Precision X-ray, Inc., North Branford, CT, USA) machine operating at 320 kvp and 12.5 mA. The dose rate at a source−subject distance of 50 cm was 260 cGy/min. The machine output was routinely calibrated using an air ionization chamber. The cells were washed with fresh medium prior to

irradiation. The cells were then radiated with X-ray irradiation at room temperature.

Clonogenic Survival Assay. Cells were seeded at various densities ranging from 100 to 100 000 cells in 4 mL of culture medium in 25 mL flasks 1 day prior to treatment. Cells were treated with therapeutics for 1 h and washed three times with fresh media after incubation. The cells were then radiated at various time points at 0, 2, 4, 5, 6, 7, 8, and 9 Gy, respectively. The cells were incubated for 10 days after irradiation. After 10 days, the cells were fixed in 50% acetone/50% methanol and stained with trypan blue. All colonies with over 50 cells were counted. The relative cell surviving fraction was calculated by dividing the number of colonies of radiated cells by the cells plated, with a correction for the plating efficiency.

***In Vivo* Tumor Assay.** Tumors were established in the left flank of Nu/Nu mice by injecting 1×10^6 KB cells in a 1:1 RPMI/Matrigel solution. Tumors were incubated for 10 days prior to treatment. Mice were treated iv with 2 mg/kg of Dtxl (whether in polysorbate form or incorporated in the equivalent amount of NT-NP or FT-NP) and subsequently irradiated using a Precision X-RAD 320 (Precision X-ray, Inc.) machine operating at 320 kvp and 12.5 mA. The dose rate at a source−subject distance of 70 cm was 50 cGy/min. Only the tumor/flank regions of the mice were irradiated, as the head and chest were protected by lead shielding. Tumor volume was measured every other day until the tumor reached 3 times the initial volume or 2 cm diameter, at which point the animal was euthanized. All animal work was approved and monitored by the University of North Carolina Animal Care and Use Committee.

Statistics. To statistically compare the change in tumor volume for mice treated with NT-NP Dtxl + XRT (3 h) and FT-NP Dtxl + XRT (3 h) groups, we chose the area under the growth curve (AUC) over the largest common observation period as an indicator of growth rate. The largest common observation period of the two groups is from time 0 to day 26. We used the trapezoidal rule to approximate AUC. On the basis of the AUCs, the Wilcoxon rank sum test was performed to compare the growth rates between the two groups. The exact one-sided *p*-value of the Wilcoxon rank sum test was calculated. Data were considered statistically significant when the *p* value was less than 0.05.

Histology. Tumors were excised from the animals at the indicated times. Samples were fixed in 2% paraformaldehyde, embedded in paraffin, and sectioned. Hematoxylin and eosin staining was performed. Images were acquired with an IX 81 microscope (Olympus) at the Microscopy Services Laboratory Core Facility at the UNC School of Medicine.

Acknowledgment. We thank Drs. J. DeSimone and R. Juliano for their guidance in conducting this work. We also thank A. Cummings for assistance with the graphics. We would also like to thank the Microscopy Services Laboratory, Animal Studies Core, and Animal Histopathology Core at the University of North Carolina for their assistance with procedures. This work was supported by grants from Golfers Against Cancer, Carolina Center for Nanotechnology Excellence Pilot Grant, and the University Cancer Research Fund from University of North Carolina. A.Z.W. is also supported by a NIH/NCI Paul Calabresi Career Development Award for Clinical Oncology K12 grant.

REFERENCES AND NOTES

1. Seiwert, T. Y.; Salama, J. K.; Vokes, E. E. The Chemoradiation Paradigm in Head and Neck Cancer. *Nat. Clin. Pract. Oncol.* **2007**, *4*, 156–171.
2. Sen, F.; Saglam, E. K.; Toker, A.; Dilege, S.; Kizir, A.; Oral, E. N.; Saip, P.; Sakallioglu, B.; Topuz, E.; Aydiner, A. Weekly Docetaxel and Cisplatin with Concomitant Radiotherapy in Addition to Surgery and/or Consolidation Chemotherapy in Stage III Non-small Cell Lung Cancer. *Cancer Chemother. Pharmacol.*
3. Karasawa, K.; Shinoda, H.; Katsui, K.; Seki, K.; Kohno, M.; Hanyu, N.; Nasu, S.; Muramatsu, H.; Maebayashi, K.; Mitsuhashi, N.; *et al*. Radiotherapy with Concurrent Docetaxel and cCarboplatin for Head and Neck Cancer. *Anticancer Res.* **2002**, *22*, 3785–3788.
4. Nabell, L.; Spencer, S. Docetaxel with Concurrent Radiotherapy in Head and Neck Cancer. *Semin. Oncol.* **2003**, *30*, 89–93.
5. ten Tije, A. J.; Verweij, J.; Loos, W. J.; Sparreboom, A. Pharmacological Effects of Formulation Vehicles: Implications for Cancer Chemotherapy. *Clin. Pharmacokinet.* **2003**, *42*, 665–685.
6. Safavy, A. Recent Developments in Taxane Drug Delivery. *Curr. Drug Delivery* **2008**, *5*, 42–54.
7. Maeda, H.; Wu, J.; Sawa, T.; Matsumura, Y.; Hori, K. Tumor Vascular Permeability and the EPR Effect in Macromolecular Therapeutics: A Review. *J. Controlled Release* **2000**, *65*, 271–284.
8. Sanna, V.; Roggio, A. M.; Posadino, A. M.; Cossu, A.; Marceddu, S.; Mariani, A.; Alzari, V.; Uzzau, S.; Pintus, G.; Sechi, M. Novel Docetaxel-Loaded Nanoparticles Based on Poly(lactide-co-caprolactone) and Poly(lactide-co-glycolide-co-caprolactone) for Prostate Cancer Treatment: Formulation, Characterization, and Cytotoxicity Studies. *Nanoscale Res. Lett.* **2011**, *6*, 260.
9. Cho, H. J.; Yoon, H. Y.; Koo, H.; Ko, S. H.; Shim, J. S.; Lee, J. H.; Kim, K.; Chan Kwon, I.; Kim, D. D. Self-assembled Nanoparticles Based on Hyaluronic Acid-Ceramide (HA-CE) and Pluronic((R)) for Tumor-Targeted Delivery of Docetaxel. *Biomaterials* **2011**, *32*, 7181–7190.
10. Chaudhari, K. R.; Ukawala, M.; Manjappa, A. S.; Kumar, A.; Mundada, P. K.; Mishra, A. K.; Mathur, R.; Monkkonen, J.; Murthy, R. S. Opsonization, Biodistribution, Cellular Uptake and Apoptosis Study of PEGylated PBCA Nanoparticle as Potential Drug Delivery Carrier. *Pharm. Res.* **2011**.
11. Liu, D.; Wang, L.; Liu, Z.; Zhang, C.; Zhang, N. Preparation, Characterization, and *in Vitro* Evaluation of Docetaxel-loaded Poly(lactic acid)-poly(ethylene glycol) Nanoparticles for Parenteral Drug Delivery. *J. Biomed. Nanotechnol.* **2010**, *6*, 675–682.
12. Enlow, E. M.; Luft, J. C.; Napier, M. E.; DeSimone, J. M. Potent Engineered PLGA Nanoparticles by Virtue of Exceptionally High Chemotherapeutic Loadings. *Nano Lett.* **2011**, *11*, 808–813.
13. Kolishetti, N.; Dhar, S.; Valencia, P. M.; Lin, L. Q.; Karnik, R.; Lippard, S. J.; Langer, R.; Farokhzad, O. C. Engineering of Self-Assembled Nanoparticle Platform for Precisely Controlled Combination Drug Therapy. *Proc. Natl. Acad. Sci. U. S. A.* **2010**, *107*, 17939–17944.
14. Luo, Y.; Ling, Y.; Guo, W.; Pang, J.; Liu, W.; Fang, Y.; Wen, X.; Wei, K.; Gao, X. Docetaxel Loaded Oleic Acid-Coated Hydroxyapatite Nanoparticles Enhance the Docetaxel-Induced Apoptosis Through Activation of Caspase-2 in Androgen Independent Prostate Cancer Cells. *J. Controlled Release* **2010**, *147*, 278–288.
15. Liu, Y.; Li, K.; Pan, J.; Liu, B.; Feng, S. S. Folic Acid Conjugated Nanoparticles of Mixed Lipid Monolayer Shell and Biodegradable Polymer Core for Targeted Delivery of Docetaxel. *Biomaterials* **2010**, *31*, 330–338.
16. Sun, B.; Feng, S. S. Trastuzumab-Functionalized Nanoparticles of Biodegradable Copolymers for Targeted Delivery of Docetaxel. *Nanomedicine (London, U.K.)* **2009**, *4*, 431–445.
17. Chan, J. M.; Zhang, L.; Yuet, K. P.; Liao, G.; Rhee, J. W.; Langer, R.; Farokhzad, O. C. PLGA-Lecithin-PEG Core-Shell Nanoparticles for Controlled Drug Delivery. *Biomaterials* **2009**, *30*, 1627–1634.
18. Service, R. F. Nanotechnology. Nanoparticle Trojan Horses Gallop from the Lab into the Clinic. *Science 330*, 314−315.
19. Koukourakis, M. I.; Giatromanolaki, A.; Pitiakoudis, M.; Kouklakis, G.; Tsoutsou, P.; Abatzoglou, I.; Panteliadou, M.; Sismanidou, K.; Sivridis, E.; Boulikas, T. Concurrent Liposomal Cisplatin (Lipoplatin), 5-fluorouracil and Radiotherapy for the Treatment of Locally Advanced Gastric Cancer: A Phase I/II Study. *Int. J. Radiat. Oncol., Biol., Phys.* **2010**, *78*, 150–155.
20. Rosenthal, D. I.; Yom, S. S.; Liu, L.; Machtay, M.; Algazy, K.; Weber, R. S.; Weinstein, G. S.; Chalian, A. A.; Mille, L. K.; Rockwell, K., Jr.; *et al*. A Phase I Study of SPI-077 (Stealth

Liposomal Cisplatin) Concurrent with Radiation Therapy for Locally Advanced Head and Neck Cancer. *Invest. New Drugs* **2002**, *20*, 343–349.
21. Wiedenmann, N.; Valdecanas, D.; Hunter, N.; Hyde, S.; Buchholz, T. A.; Milas, L.; Mason, K. A. 130-nm Albumin-Bound Paclitaxel Enhances Tumor Radiocurability and Therapeutic Gain. *Clin. Cancer Res.* **2007**, *13*, 1868–1874.
22. Parker, N.; Turk, M. J.; Westrick, E.; Lewis, J. D.; Low, P. S.; Leamon, C. P. Folate Receptor Expression in Carcinomas and Normal Tissues Determined by a Quantitative Radioligand Binding Assay. *Anal. Biochem.* **2005**, *338*, 284–293.
23. Saba, N. F.; Wang, X.; Muller, S.; Tighiouart, M.; Cho, K.; Nie, S.; Chen, Z. G.; Shin, D. M. Examining Expression of Folate Receptor in Squamous Cell Carcinoma of the Head and Neck as a Target for a Novel Nanotherapeutic Drug. *Head Neck* **2008**.
24. Zhang, L.; Chan, J. M.; Gu, F. X.; Rhee, J. W.; Wang, A. Z.; Radovic-Moreno, A. F.; Alexis, F.; Langer, R.; Farokhzad, O. C. Self-Assembled Lipid−Polymer Hybrid Nanoparticles: A Robust Drug Delivery Platform. *ACS Nano* **2008**, *2*, 1696–1702.
25. Edelman, M. J. Novel Taxane Formulations and Microtubule-binding Agents in Non-small-cell Lung Cancer. *Clin. Lung Cancer* **2009**, *10*), S30–34.
26. Lu, J. M.; Wang, X.; Marin-Muller, C.; Wang, H.; Lin, P. H.; Yao, Q.; Chen, C. Current Advances in Research and Clinical Applications of PLGA-Based Nanotechnology. *Expert Rev. Mol. Diagn.* **2009**, *9*, 325–341.
27. Gabizon, A. A.; Shmeeda, H.; Zalipsky, S. Pros and Cons of the Liposome Platform in Cancer Drug Targeting. *J. Liposome Res.* **2006**, *16*, 175–183.
28. Kim, T. Y.; Kim, D. W.; Chung, J. Y.; Shin, S. G.; Kim, S. C.; Heo, D. S.; Kim, N. K.; Bang, Y. J. Phase I and Pharmacokinetic Study of Genexol-PM, a Cremophor-Free, Polymeric Micelle-Formulated Paclitaxel, in Patients with Advanced Malignancies. *Clin. Cancer Res.* **2004**, *10*, 3708–3716.
29. Matsumura, Y.; Kataoka, K. Preclinical and Clinical Studies of Anticancer Agent-Incorporating Polymer Micelles. *Cancer Sci.* **2009**, *100*, 572–579.
30. Bagalkot, V.; Farokhzad, O. C.; Langer, R.; Jon, S. An Aptamer-Doxorubicin Physical Conjugate as a Novel Targeted Drug-Delivery Platform. *Angew. Chem., Int. Ed.* **2006**, *45*, 8149–8152.
31. Wang, A. Z.; Bagalkot, V.; Vasilliou, C. C.; Gu, F.; Alexis, F.; Zhang, L.; Shaikh, M.; Yuet, K.; Cima, M. J.; Langer, R.; *et al*. Superparamagnetic Iron Oxide Nanoparticle-Aptamer Bioconjugates for Combined Prostate Cancer Imaging and Therapy. *ChemMedChem* **2008**, *3*, 1311–1315.
32. Hermens, A. F.; Barendsen, G. W. Changes of Cell Proliferation Characteristics in a Rat Rhabdomyosarcoma Before and After X-irradiation. *Eur. J. Cancer* **1969**, *5*, 173–189.
33. Stephens, T. C.; Currie, G. A.; Peacock, J. H. Repopulation of Gamma-Irradiated Lewis Lung Carcinoma by Malignant Cells and Host Macrophage Progenitors. *Br. J. Cancer* **1978**, *38*, 573–582.
34. Huang, Q.; Li, F.; Liu, X.; Li, W.; Shi, W.; Liu, F. F.; O'Sullivan, B.; He, Z.; Peng, Y.; Tan, A. C.; *et al*. Caspase 3-Mediated Stimulation of Tumor Cell Repopulation during Cancer Radiotherapy. *Nat. Med. (N.Y., U.S.)* **2011**, *17*, 860–866.